Texila International Journal of Public Health
ISSN: 2520-3134
DOI: 10.21522/TIJPH.2013.12.02.Art033

Evaluation of Physical and Mechanical Properties of a Novel Titanium Dioxide Nanoparticle Infiltrated Orthodontic Adhesive – An *In-Vitro* Study

Harsha L, Aravind Kumar Subramanian*
Department of Orthodontics, Saveetha Dental College and Hospitals, Saveetha Institute of Medical and Technical Sciences, Saveetha University, Chennai–600077, India

Abstract

This in-vitro study aims to assess and compare the physical and mechanical properties of a green synthesized (novel) Titanium dioxide nanoparticle infiltrated orthodontic adhesive with conventional orthodontic adhesive. A total of twenty disk-shaped specimens were fabricated by condensing the composite resin in a stainless-steel metal mold having a circular shape (10 x 2 mm) and polymerizing it using blue light (470nm). Scanning Electron Microscopy (SEM) and Fourier-transform infrared spectroscopy (FTIR) were used to characterize the TiO_2 NPs. The results of physical properties such as colour stability, and surface roughness showed no significant mean difference and the microhardness of two orthodontic adhesives showed a significantly greater hardness for conventional adhesives. Conventional orthodontic adhesive showed significantly increased compressive strength and greater tensile strength for novel TiO_2-NPs infiltrated orthodontic adhesive ($p>0.05$). The results also showed improved mechanical properties for both groups.

Keywords: *Green Synthesis, Mechanical Properties, Nanoparticles, Orthodontic Adhesives, Physical, Titanium Dioxide.*

Introduction

A big challenge in orthodontic treatment for both patients and orthodontists with fixed orthodontic appliances is maintaining good oral hygiene, as fixed appliance components are plaque-retentive [1, 2]. Following this big challenge, occurs enamel demineralization during and after orthodontic treatment resulting in white spot lesions (WSLs). It has been reported that WSLs occur in 30% to 70% of the patients during orthodontic treatment [3-5] with a prevalence rate of 68.4% [6], affecting 18.5% of tooth surfaces [7]. These lesions are induced clinically within 4 weeks of orthodontic treatment occurring due to decreased oral pH and lactic acid produced by *Streptococcus mutans* [8-11]. Thus, the prevention of WSLs becomes inevitable to provide the integrity of dentition during orthodontic treatment [12].

This lesion can be managed by maintaining good oral hygiene, and use of topical fluorides including high-fluoridated toothpastes, fluoride, chlorohexidine mouthwashes, gels, and varnishes. Patient cooperation is of utmost importance in carrying out these preventive strategies, which is questionable. Short-term release of antimicrobial agents with reduced mechanical, and physical properties and possible tooth discolouration are some of the demerits of these preventive strategies [12, 13]. Thus, there is a need to produce agents with superior mechanical, chemical, physical, optical, and antimicrobial properties.

Recently, research has been directed at producing orthodontic adhesives with high antimicrobial properties to prevent WSLs. High charge density and large surface area of nanoparticles (NPs) which interact with bacterial cells exhibiting increased

Received: 10.06.2024 ***Accepted: 17.06.2024*** ***Published on: 28.06.2024***
****Corresponding Author: aravindkumar@saveetha.com***

antimicrobial efficacy are being introduced into the orthodontic adhesives without affecting the value of the bonded interface [14-18]. Nanoparticles such as gold [19], silver [20], copper [21], zinc oxide [22], silicon dioxide [23, 24], hydroxyapatite [25], and titanium dioxide (TiO_2) [26] have been added to orthodontic adhesive to prevent WSLs.

Compared to other NPs, Titanium dioxide nanoparticles are considered to have increased optical properties with a high reflective index, and chemical stability causing no colour change of resin composites around brackets. Also, TiO_2 has excellent mechanical properties such as increased microhardness, flexural strength, shear bond strength and modulus of elasticity [27-33]. Apart from augmented mechanical properties, TiO_2 NPs infiltrated into orthodontic adhesives display compelling antimicrobial properties without affecting the bond strength [34].

Nanoparticles are usually synthesized by chemical methods causing environmental pollution, increased energy consumption and imposing health problems. Green synthesis is the novelty which uses reducing agents derived from plants or microorganism extracts to reduce the metal ions, combating the above-mentioned problems [35]. Green synthesis costs less, decreases environmental pollution and improves human health and safety.

Though earlier studies assessed the mechanical properties of TiO_2 NPs, a literature search showed none of the studies assessed the physical and mechanical properties of green synthesized TiO_2 NPs infiltrated orthodontic adhesives. Thus, the present in-vitro study aims to assess and compare the physical and mechanical properties of a green synthesized (novel) Titanium dioxide nanoparticle infiltrated orthodontic adhesive with conventional orthodontic adhesive.

Materials and Methods

Sample Size Calculation

Based on the previous study [36], a sample size of 10 specimens per group was needed to exhibit a statistically significant difference in mechanical and physical properties between the groups upon alpha error of 5% and power of 80%.

Preparation of Titanium Dioxide Nanoparticle

Preparation of Leaf Extract

One gram of *Eucalyptus globulus* powder was mixed with 100 ml of distilled water to form a homogenous mix of the plant extract. The solution was then heated and boiled in a heating mantle. Using Whatman no:1 filter paper, the boiled plant extract was filtered, and the supernatant solution was collected in a beaker.

Preparation of TiO_2 NPs

About 50 ml of distilled water was mixed with 0.39g of titanium dioxide powder. To this, 50 ml of the prepared supernatant plant extract solution was added. The obtained solution was then placed on a magnetic stirrer/ orbital shaker overnight to observe the visual and chemical changes observed during the synthesis of TiO_2 nanoparticles. A colour change from white to whitish brown was observed. This was due to the reduction of the metal ion ($Ti4^{+}$) indicating the synthesis of TiO_2 nanoparticles. Using hourly UV-vis spectrometric data, titanium dioxide nanoparticle production was evaluated and the same was used to confirm the presence of TiO_2 nanoparticles produced in the solution.

Upon confirmation, the solution was equally divided and poured into centrifuge tubes for centrifugation. The pellet obtained was collected in a separate tube and later poured into petri dishes. These Petri dishes were dried in a hot air oven, the dry substrate containing the TiO_2 nanoparticle was scraped, and the powder was collected and labelled.

Characterization of Synthesized TiO_2 Nps Using Scanning Electron Microscopy (Sem) and Fourier-Transform Infrared Spectroscopy (FTIR)

Scanning Electron Microscopy SEM

The JSM –IT800 Nano SEM (Joel, Nagoya University, Japan) was used to view the obtained nanoparticle and confirm its shape and size. SEM was used to examine external specifications of adsorbent morphology.

UV-Vis Spectroscopy

UV-Vis Spectroscopy (Malvern Panalytical Ltd; Enigma Business Park, Grovewood Road, Malvern WR14 1XZ, United Kingdom) was used to record the synthesized titanium dioxide nanoparticles' UV-Vis peak of absorption. The specimens' scanning ranged from 350 to 660 nm. A distilled water standard was used to interpret all UV-Vis absorption spectra.

FT-IR

An FTIR spectrophotometer (BRUKER; Massachusetts; United States) was used to study the functional groups on the biaxial surface. It is a good analytical tool to illustrate the bending properties of synthesized nanoparticles. The spectrum was recorded in the range of 400–4000 cm.

Preparation and Characterization of TiO_2 Infiltrated Orthodontic Adhesive

Preparation of Nano Infiltrated Adhesive

To achieve an orthodontic adhesive containing 1% nanoparticle, 0.04g of prepared titanium dioxide nanoparticle was mixed with 4 ml of dichloromethane (DCM) in a beaker. The beaker was covered with aluminium foil all around to ensure that no light passed through. To this mixture, 4g of orthodontic adhesive (Ormco Enlight light-cured adhesive, ORMCO) was added and continuously stirred manually. The beaker was then placed in an orbital shaker with an rpm (rotations per minute) of 500 for 24 hours to ensure uniform distribution of nanoparticles within the matrix. The obtained material was then retro-filled into a black syringe to prevent light exposure.

Characterization of TiO_2 Nanoparticle Infiltrated Orthodontic Adhesive

The JSM –IT800 Nano SEM and EDX (Energy Dispersive X-ray) were used to view the obtained nanoparticle infiltrated orthodontic adhesive and confirm its shape and size. SEM was used to examine external specifications of adsorbent morphology.

Evaluation of Properties of the Novel TiO_2 Nanoparticle Infiltrated Orthodontic Adhesive

Grouping of Specimens

All tests evaluating the physical, chemical, and mechanical properties were conducted between two sample groups, Group 1 (G1): Conventional orthodontic adhesive (ENLIGHT ORMCO), Group 2 (G2): Titanium dioxide infiltrated orthodontic adhesive (TiO2 nanoparticle + Enlight orthodontic adhesive).

Physical Properties

All physical and mechanical properties were measured before and after the ageing of the study material.

Ageing Procedure

All specimens of Groups 1 and 2 were subjected to thermo-cycling by being stored alternatively in water reservoirs at 5°C and 55°C, respectively, and remaining in each reservoir for 30 seconds.

Specimen Preparation

A total of twenty disk-shaped specimens were fabricated by condensing the composite resin in a stainless-steel metal mold having a circular shape (10 x 2 mm) and polymerizing it using blue light (470nm). Following polymerization, the specimens were removed from the mold and polished with a Sof-Lex polishing kit (3M ESPE). A digital calliper was used to check the specimen's dimensions. The specimens with voids, defects, or incorrect dimensions were discarded. Specimens were then stored for 24 hours in distilled water in a dark container, at room temperature for complete polymerization. These prepared samples were used for evaluating the colour stability, surface roughness, and hardness before and after ageing.

Colour

Colour measurements were performed with a SPECTROPHOTOMETER CM–5 according to the CIELab (Commission Internationale de l'Eclairage, L*, a*, b*) coordinates. The target mask is selected based on the illumination area (specimen measuring port size) of 3 mm, and zero calibration is performed to compensate for the effects of stay light. The colour coordinates L, a and b of each specimen were measured relative to the standard illumination D65 and a 10-degree standard observer.

The CIELab coordinates were used to calculate the colour difference (ΔE) between the "before" and "after" periods of thermocycling. The colour difference (ΔE) between the two-time interval readings was calculated according to the following equation:

$$\sqrt{(\Delta L)^2 + (\Delta a)^2 + (\Delta b)^2} = \Delta E^2$$

Where ΔL, Δa, and Δb are the differences between the parameters before and after thermocycling. $\Delta E < 1$ were considered clinically imperceptible, between 1 to 3.3 as acceptable colour change, >3.3 were considered clinically relevant and highly noticeable.

Surface Roughness

The surface roughness parameters of the specimens were evaluated using Surftest SJ-310 (Mitutoyo South Asia Pvt. Ltd, New Delhi). The surface profile was determined as average roughness (Ra), defined as the mean between peaks and valleys of the surface profile, Rq is the largest roughness considering all the cut-offs (Highest peak and highest valley), and Rz is the mean of 10 peaks and 10 valley heights in each cut-off. Ra and Rz are average roughness parameters, and they are not enough to distinguish surfaces that differ in spacing or shape. Data for the surface roughness of all specimens before and after thermocycling were recorded separately for Ra, Rq and Rz.

Hardness

The Vickers hardness of the specimens was evaluated with a microhardness tester (Shimadzu HMV-G, Newage Testing Instruments, Southampton, PA). The indentations were made with a Vickers diamond indenter at a weight of HV 0.3 (2.942 N) with a dwell time of 20 seconds. The indentation was captured at a magnification of 40X. The values were noted for each of the specimens subjected to testing.

Mechanical Properties

Compressive and Diametral Tensile Strength

Mold Construction

A 3 mm diameter by 10 mm height cylindrical Teflon mold was fabricated according to International Standards Organization (ISO) No. 9917 (2000).

Specimen Preparation

The orthodontic Adhesive was condensed in the Teflon mold, which was then placed on a glass plate according to each group. Specimens were covered with celluloid strips and pressed with another glass plate. All the specimens were exposed to light cure for 40 seconds on both sides. The specimens were stored in distilled water for 24 hours before testing.

Compressive Strength Testing

Specimens were loaded on the Universal testing machine at a crosshead speed of 0.5 mm/min. The specimens were placed with their flat ends vertically laid between the two metal plates. The load was applied until the specimen was crushed; the peak force required to fracture each specimen was recorded in Newton from the stress-strain curve. The compressive strength was calculated in megapascals (MPa) using the following equation

$$4P = \pi d$$

Where P is the load at the fracture point in Newtons and d is the diameter of the specimen.

Diametric Tensile Strength

Measuring the tensile strength of orthodontic adhesive is done using an indirect tensile test, in which a compressive load is placed on the diameter of a cylindrical specimen. The compressive strength induces a tensile stress in the plane of the application of the force. The tensile strength is directly proportional to the compressive load. In this test, the specimen cylinder was mounted on the universal testing machine and the load was applied to the specimen using a crosshead speed of 0.5 mm/min applying a compressive force to the specimen until fracture. The diametral tensile strength was calculated in MPa using the following equation

$$2P = \pi dt$$

Where P is the load at the fracture point in Newtons, d is the diameter of the specimen, and t is the thickness of the specimen.

Statistical Analysis

Data was collected and tabulated in Microsoft Excel and imported for statistical analysis to SPSS software (Statistical Package for the Social Sciences Inc. IBM, NY, USA) version 24.0. The normal distribution of the data was evaluated using Shapiro-Wilk's test. The data was normally distributed, hence parametric tests were used. Independent t-tests and paired t-tests were used to compare colour stability, surface roughness, hardness, compressive strength and diametral strength between and within the groups respectively. A significance level of $p < 0.05$ was considered.

Results

Green synthesis of TiO2 NPs

A colour change from white to whitish brown was observed, as shown in Figure 1. This was due to the reduction of the metal ion (Ti4+) indicating the synthesis of TiO_2 nanoparticles. UV-vis spectrometry was used and confirmed the presence of TiO_2 nanoparticles in the solution.

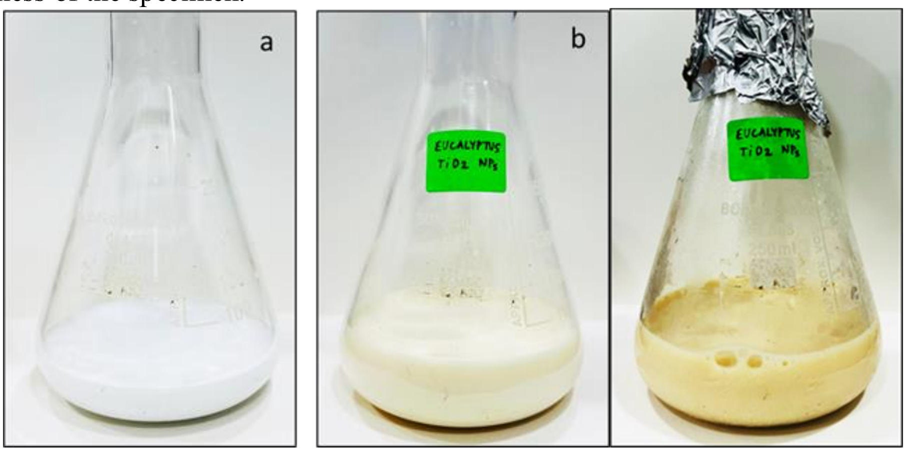

Figure 1. (a) TiO2 Mixture with Distilled Water; (b) TiO2 Solution Mixed with the Plant Extract

Characterization of TiO_2 NPs

The present study has described the synthesis of TiO_2 NPs by Eucalyptus globulus leaf extract mediated reduction of aqueous titanium ions. The formation of TiO_2 NPs in aqueous solutions was confirmed by using UV-visible spectral analysis. Results showed the reduction of titanium ions, and the generation of TiO_2 NPs was completed after overnight incubation at room temperature. The formation of a whitish-brown colour indicated the reduction of titanium ions. The absorption spectra of had absorbance peaks between 300-350 nm for the plant extract solution exposed to TiO_2 (Figure 2).

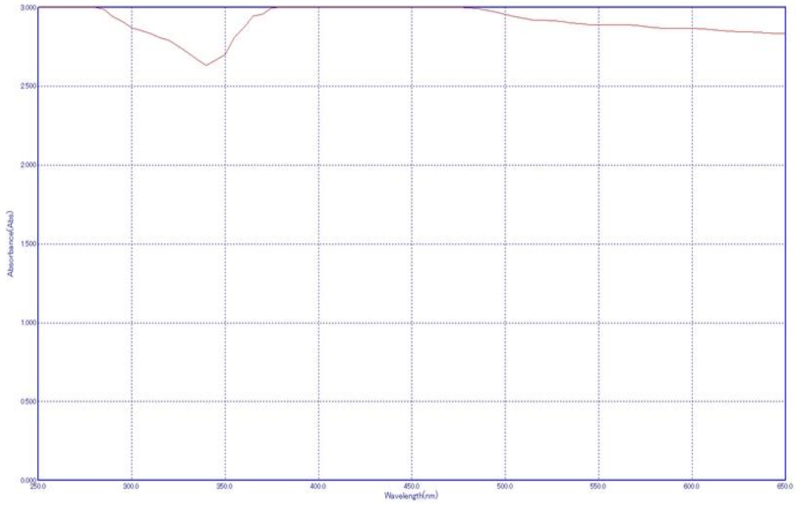

Figure 2. Uv-Vis Spectroscopy Graph

FT-IR

Estimation of bending properties of the TiO_2 NPs was done at room temperature between the wavelengths 400-4000 cm^{-1}. It can be observed that at 584.24 cm^{-1} TiO_2 bending mode and at 1101.46 cm^{-1} stretching mode can be observed (Figure 3). This may be attributed to surface water sorption.

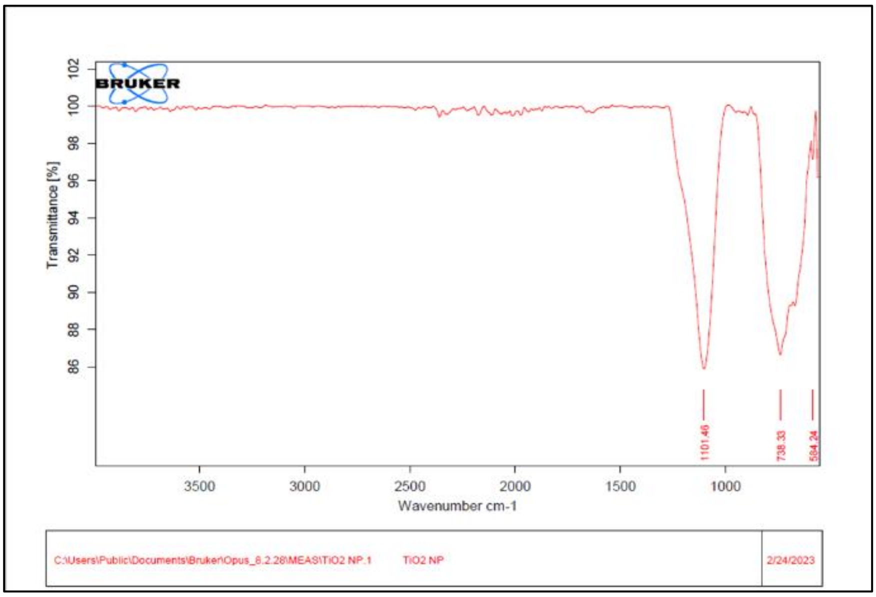

Figure 3. Ftir Graphic Representation

SEM and EDX

The scanning electron microscope was used to evaluate the size, shape, and surface properties, like morphology. SEM picture at 10x magnification of TiO_2 nanoparticles synthesized using the leaf extract of Eucalyptus Globulus. The SEM image shows a uniform distribution of the TiO_2 nanoparticles, which are smooth and spherical (Figure 4). The average size of the nanoparticle ranged between 20 and 70 nm.

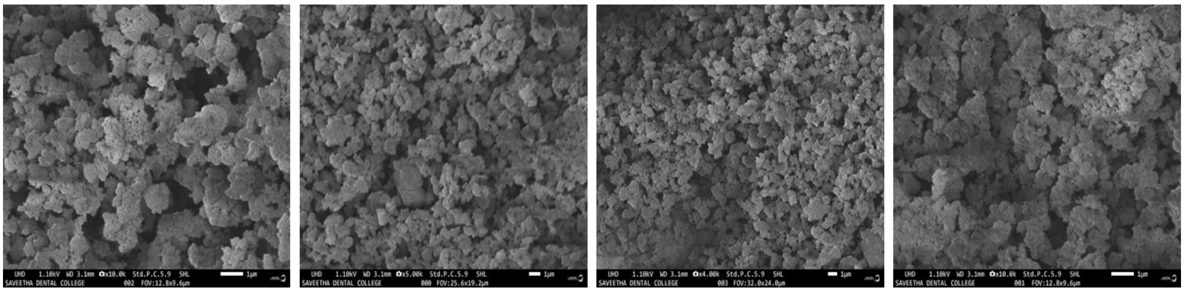

Figure 4. Sem Images of Tio2 Nanoparticle

EDX profile contained a strong TiO_2 signal along with other weak signals, which might be due to the biomolecules bound to the surface of the nanoparticles. Although strong signals were due to titanium in the nanoparticles, weaker signals for oxygen and chloride were due to the biomolecules of *Eucalyptus globulus*. The signals might have been due to X-ray emission from carbohydrates/proteins/enzymes existing in the cell wall of the biomass. In the present study, TiO_2 NPs revealed a strong absorption spectrum at 4-5 keV (Figure 5).

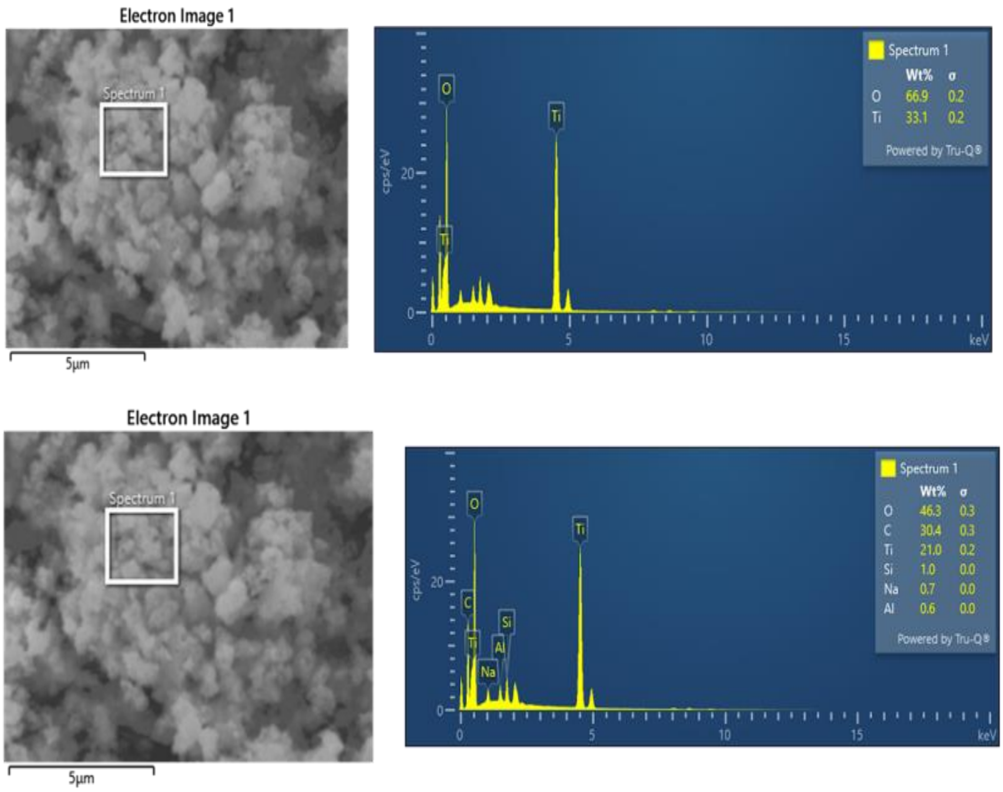

Figure 5. Edx Images of Tio2 Nanoparticle

Characterization of Novel Tio2 Infiltrated Orthodontic Adhesive

SEM/EDX

The scanning electron microscope was used to evaluate the dispersion of TiO_2 NPs in the orthodontic adhesive matrix. Figure 6 illustrates the SEM picture at 10x magnification of TiO_2 nanoparticles infiltrating orthodontic adhesive. The SEM image shows a uniform distribution of the TiO_2 nanoparticles that are smooth and spherical. The average size of the nanoparticle ranges between 20 and 70 nm.

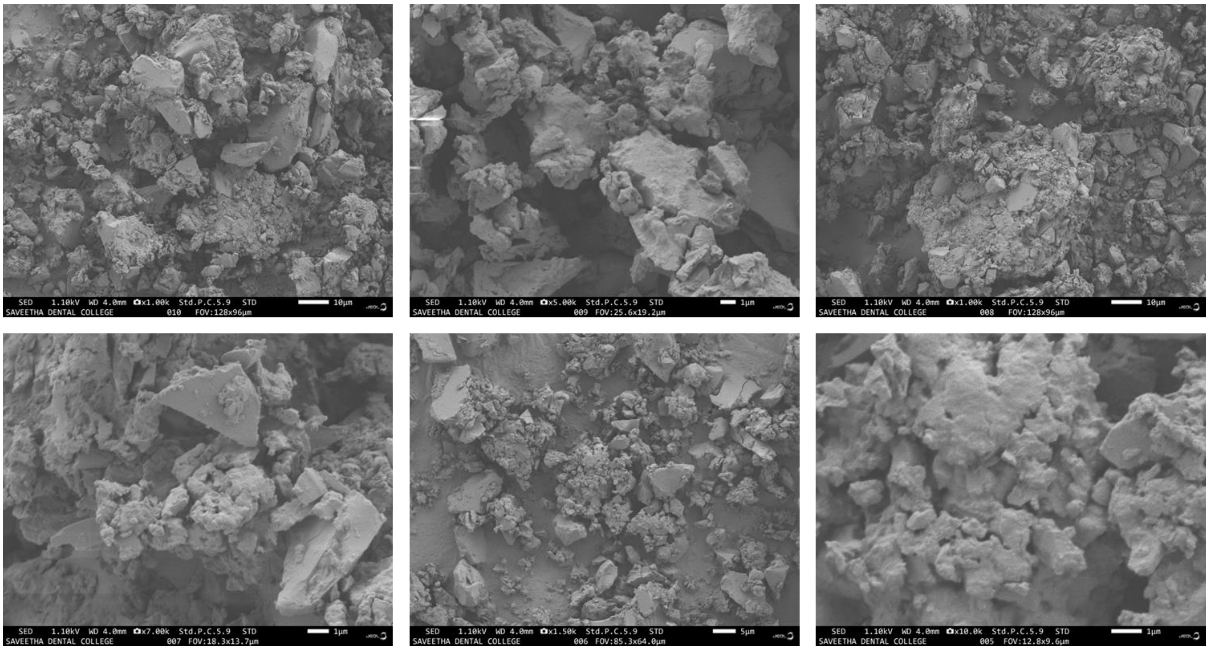

Figure 6. SEM Images of TiO_2 Nanoparticle Infiltrated Orthodontic Adhesive

The analysis of the TiO_2 nanoparticles infiltrated orthodontic adhesive by EDX showed the presence of titanium (Figure 7). The EDX profile contained a strong titanium dioxide signal along with other weak signals, which might be due to the biomolecules bound to the surface of the NPs. Although strong signals were due to titanium in the nanoparticles, weaker signals for oxygen and chloride were due to other biomolecules. The signals might have been due to X-ray emission from carbohydrates/proteins/enzymes existing in the cell wall of the biomass. In the present study, TiO_2 nanoparticles infiltrated orthodontic adhesive and revealed a strong absorption spectrum at 4-5 keV.

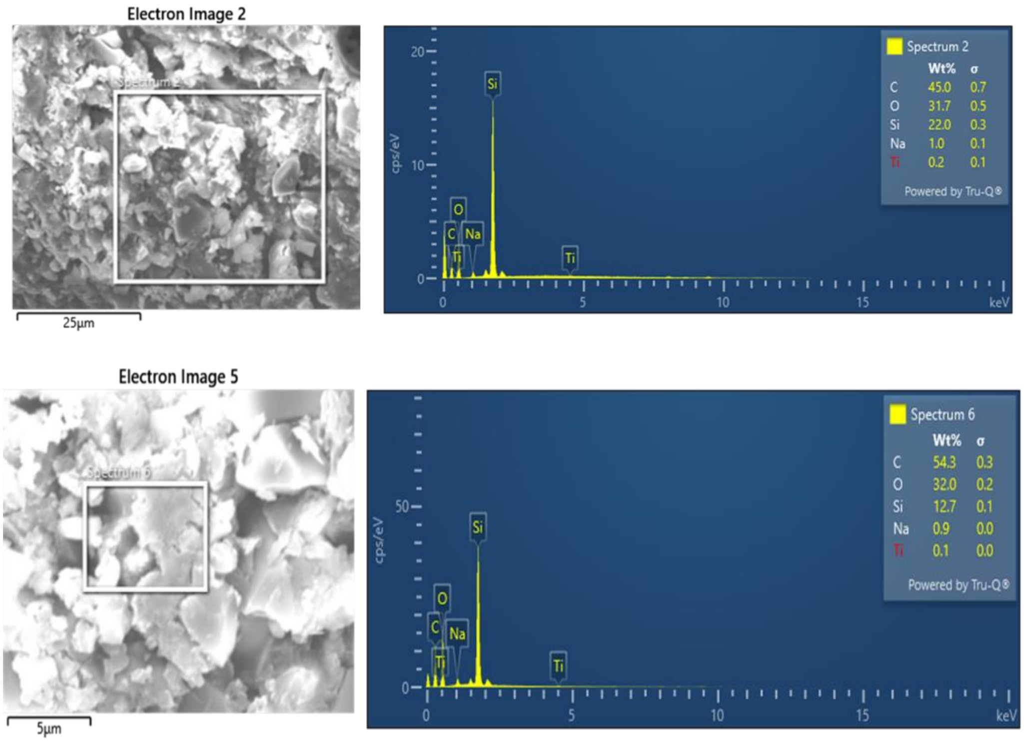

Figure 7. EDX Images of TiO_2 Nanoparticle Infiltrated Orthodontic Adhesive

Physical Properties

Colour Stability

The mean comparison of ΔE values is presented in Table 1. No statistically significant mean difference was observed between the two groups (P > 0.05). Conventional orthodontic adhesive (ΔE =1.71± 0.80) showed lower ΔE values when compared to TiO_2 infiltrated orthodontic adhesive (2.2 ± 1.1). ΔE values of both groups appear to be within the clinically acceptable range (ΔE<3.3).

Table 1. Comparison of Color Stability Values between the Study Groups

Color Stability	*Mean ± SD*		*p value*
	Group 1 (10)	*Group 2 (10)*	
ΔE value	*1.71 ± 0.80*	*2.2 ± 1.1*	*0.248*

Independent t test

Surface Roughness

Comparison of mean Ra, Rq and Rz parameters showed no statistically significant difference in surface roughness between (p>0.05). No statistically significant difference was elucidated within the groups before and after thermocycling (Table 2).

Table 2. Mean Comparison of Surface Roughness among the Study Groups

Surface roughness	*Thermocycling*	*Mean ± SD*		*p value*
		Group 1	*Group 2*	
Ra (nm)	*Before*	*0.23 ± 0.07*	*0.47 ± 0.21*	*0.004**
	After	*0.25 ± 0.06*	*0.41 ± 0.11*	*0.001**
p value		*0.428#*	*0.428#*	
Rq (nm)	*Before*	*0.32 ± 0.10*	*0.63 ± 0.28*	*0.005**
	After	*0.36 ± 0.09*	*0.54 ± 0.15*	*0.004**
p-value		*0.315#*	*0.498#*	
Rz (nm)	*Before*	*1.82 ± 0.51*	*3.53 ± 1.32*	*0.001**
	After	*2.21 ± 0.68*	*3.01 ± 0.82*	*0.029**
p-value		*0.111#*	*0.415#*	

* Independent t test; # Paired t test

Hardness

Table 3 shows the mean comparison of microhardness between two adhesives. There is a significant mean difference in microhardness between the adhesives (p<0.05). However, no statistically significant difference was observed within the adhesives (before and after thermocycling). Conventional orthodontic adhesive had a greater hardness value (HV) than TiO_2-infiltrated orthodontic adhesive and the hardness value increased in both groups after thermocycling.

Table 3. Comparison of Mean Hardness between and Within the Groups

Microhardness	*Thermocycling*	*Mean ± SD*		*p value*
		Group 1	*Group 2*	
	Before	*54.21 ± 6.70*	*44.64 ± 8.21*	*0.011**
	After	*59.33 ± 15.4*	*47.19 ± 8.63*	*0.044**
p value		*0.306#*	*0.294#*	

* Independent t test; # Paired t test

Mechanical Properties

Compressive and Diametral Tensile Strength

Conventional and TiO_2 infiltrated Orthodontic adhesives showed no statistically significant difference in their compressive and tensile strengths ($p>0.05$). Conventional orthodontic adhesive had an increased compressive strength when compared to TiO_2-infiltrated orthodontic adhesive, while the result was vice versa for diametral tensile strength (Table 4).

Table 4. Mean Comparison of Compressive and Diametral Tensile Strength in MPA between the Study Groups

Mechanical properties	**Mean ± SD**		**p value**
	Group 1 (10)	**Group 2 (10)**	
Compressive strength (MPa)	202.39 ± 47.10	187.69 ± 38.73	0.456
Diametral tensile strength (MPa)	118.58 ± 22.71	125.14 ± 25.68	0.533

Independent t-test

Discussion

There is no literature explaining the efficacy of green synthesized TiO_2 NPs infiltrated orthodontic adhesives to prevent WSLs compared with conventional orthodontic adhesives. This in-vitro study investigated and compared the physical and mechanical properties of green synthesized TiO_2 NPs infiltrated orthodontic adhesives. The outcomes of physical properties such as colour stability and surface roughness of novel TiO_2 infiltrated orthodontic adhesives were significantly like that of conventional orthodontic adhesives. The hardness of conventional orthodontic adhesives was found to be significantly higher than that of novel TiO2-infiltrated orthodontic adhesives. Similarly, the mechanical properties of novel TiO2-infiltrated orthodontic adhesives are significantly like conventional orthodontic adhesives.

As the present study is an in-vitro study, doubt may arise that thermal stresses may affect the physical and mechanical properties of orthodontic adhesives when used in the oral cavity. To overcome this problem, thermocycling, a laboratory procedure of exposing dental materials to temperature ranges which are like those occurring in the oral cavity is carried out for both conventional and novel TiO2-infiltrated orthodontic adhesives [37, 38].

Scanning Electron Microscope

SEM images of *Eucalyptus globulus* leaf extracted TiO_2 NPs and infiltrated orthodontic adhesive showed uniform distribution which is smooth and spherical. The average nanoparticle size ranged between 20 – 70 nm which is inconsistent with the TiO_2 NPs prepared from jasmine flower and Aloe Vera whose average NPs size ranged between 32-48 nm [39, 40]. Decreased particle size is inversely proportional to the surface volume of the material. Thus, they easily bond to the tooth surface and penetrate bacterial surfaces and decompose them [41].

Energy Dispersive X Ray Analysis

EDX analysis of green synthesized TiO_2 NPs and TiO_2 infiltrated orthodontic adhesive showed strong titanium signals and weak oxygen and chloride signals with the absorption spectrum of TiO_2 NPs at 4-5 KeV. These strong and weak signals might be due to phytoconstituents from Eucalyptus leaf extract. This absorption spectrum is like the TiO_2 NPs synthesized from *Ocimum sanctum* leaf extract and *Sesbania grandiflora* leaf extract used to heal diabetic wounds [42, 43].

Fourier-Transform Infrared Spectroscopy

In the FTIR spectra showed a peak at 584.24 cm^{-1} for bending mode and peak at 1101.46 cm^{-1} for the stretching mode of TiO_2 NPs. This result is similar to the peak of TiO_2 NPs synthesized from *Ocimum sanctum* leaf extract was 590 cm^{-1} which is used to heal diabetic wounds [42]. This peak at FTIR spectra of TiO_2 is due to the Ti – O -O bond [44].

Colour Stability

Green synthesized TiO_2 NPs infiltrated orthodontic adhesives from Eucalyptus leaf extract showed a color stability ΔE value of 2.2 ± 1.1 which is similar to the ΔE value of conventional orthodontic adhesives (1.71± 0.80). These ΔE values are up to the acceptable range as reported in an in-vitro study of composite resins [45].

Surface Roughness

Results of Ra, Rq and Rz values of both the orthodontic adhesives before and after thermocycling showed no significant difference. In contrast to this result, an in-vitro study that evaluated the surface roughness of TiO_2 NPs to the heat cured denture-based resin reported increased mean surface roughness [46].

Hardness

The microhardness of two orthodontic adhesives showed a significant greater hardness for conventional orthodontic adhesives. Thermocycling has not affected the hardness of both orthodontic adhesives. A study on the hardness of TiO_2 nanotubes added to polycrystalline hydroxyapatite bio ceramic from bovine bones showed increased hardness [47]. Although chemically extracted TiO_2 nanoparticles increased the hardness, the constituents of Eucalyptus leaf extract would have reduced the hardness.

Compressive and Tensile Strength

Conventional orthodontic adhesives showed significantly increased compressive strength while novel TiO_2 infiltrated orthodontic adhesives had significant high tensile strength. An in-vitro study which evaluated 1% TiO_2 NPs infiltrated orthodontic adhesives showed high compressive and tensile strength [48]. As mentioned earlier, the constituents of Eucalyptus leaf extract would have reduced the compressive strength.

Strength and Limitations

This is the first study to evaluate the physical and mechanical properties of green synthesized TiO_2 nanoparticle-infiltrated orthodontic adhesives. The strength of the in-vitro study is that its design completely simulates in-vivo oral cavity temperatures by thermocycling. Though thermocycling is done to simulate the oral cavity temperatures, factors such as patients' dietary habits and oral hygiene which may influence the study outcomes are not considered. Further, the influence of saliva on the properties of green synthesized TiO_2 nanoparticle infiltrated orthodontic adhesives has not been assessed. Thus, in-vivo studies to assess their clinical applicability and efficacy are needed. Also, identification of proper concentration of TiO_2 NPs is recommended.

Conclusions

Mean color stability and surface roughness was similar in both orthodontic adhesives. High mean hardness was recorded in conventional orthodontic adhesives. The results of mechanical properties showed greater compressive strength for conventional orthodontic adhesives and greater tensile strength for novel TiO_2 NPs infiltrated orthodontic adhesives. Overall, the present in-vitro findings showed improved physical and mechanical properties of novel TiO2 NPs infiltrated orthodontic adhesives.

References

[1]. Sruthi, M. A., Gurunathan, D., 2022, An Evidence-Based Classification on the Location of White Spot Lesions in Primary Teeth: A Pilot Study. *World Journal of Dentistry.* Apr 11;13(3):261-5. https://www.wjoud.com/doi/WJOUD/pdf/10.5005/jp-journals-10015-2044

[2]. Verma, P., Jain, R. K., 2022. Visual Assessment of Extent of White Spot Lesions in Subjects Treated with Fixed Orthodontic Appliances: A Retrospective Study. *World Journal of Dentistry*. May;13(3):246. https://www.wjoud.com/doi/WJOUD/pdf/10.5005/jp-journals-10015-2042

[3]. Richter, A. E., Arruda, A. O., Peters, M. C., Sohn, W., 2011., Incidence of Caries Lesions Among Patients Treated with Comprehensive Orthodontics, *Am. J. Orthod. Dentofac. Orthop.,* 139, 657–664, https://www.academia.edu/download/69601667/j.ajodo.2009.06.03720210913-11024-bqhi9r.pdf

[4]. Tufekci, E., Dixon, J. S., Gunsolley, J. C., Lindauer, S. J., 2011, Prevalence of White Spot Lesions During Orthodontic Treatment with Fixed Appliances, *Angle Orthod.*, 81, 206–210, https://meridian.allenpress.com/angle-orthodontist/article-pdf/81/2/206/1390940/051710-262_1.pdf

[5]. Julien, K. C., Buschang, P. H., Campbell, P. M., 2013, Prevalence of White Spot Lesion Formation During Orthodontic Treatment, *Angle Orthod*, 83 , 641–7, https://meridian.allenpress.com/angle-orthodontist/article-pdf/83/4/641/1394555/071712-584_1.pdf

[6]. Sundararaj, D., Venkatachalapathy, S., Tandon, A., Pereira, A., 2015, Critical Evaluation of Incidence and Prevalence of White Spot Lesions During Fixed Orthodontic Appliance Treatment: A Meta-Analysis, *J Int Soc Prev Community Dent*, 5:433–9, https://journals.lww.com/jpcd/fulltext/2015/05060/Critical_evaluation_of_incidence_and_prevalence_of.1.aspx

[7]. Srivastava, K., Tikku, T., Khanna, R., Sachan, K., 2013, Risk Factors and Management of White Spot Lesions in Orthodontics, *J. Orthod. Sci,* 2:43–49, https://journals.lww.com/jpcd/fulltext/2015/05060/Critical_evaluation_of_incidence_and_prevalence_of.1.aspx

[8]. Asiry, M. A., Alshahrani, I., Alqahtani, N. D., Durgesh, B., 2019, Efficacy of Yttrium (Iii) Fluoride Nanoparticles in Orthodontic Bonding, *J. Nanosci. Nanotechnol,* 19, 1105–1110, https://doi.org/10.1166/jnn.2019.15894

[9]. Assery, M., Ajwa, N., Alshamrani, A., Alanazi, B., Durgesh, B., Matinlinna, J., 2019 , Titanium Dioxide Nanoparticles Reinforced Experimental Resin Composite for Orthodontic Bonding, *Mater. Res. Express,* 6, 125098, 10.1088/2053-1591/ab5a93

[10]. Durgesh, B. H., Alkheraif, A. A., Pavithra, D., Hashem, M. I., Alkhudhairy, F., Elsharawy, 2017,

Evaluation of an Experimental Adhesive Resin for Orthodontic Bonding, *Mech. Compos. Mater*, 53, 389–398, https://doi.org/10.1007/s11029-017-9670-z

[11]. Poosti, M., Ramazanzadeh, B., Zebarjad, M., Javadzadeh, P., Naderinasab, M., Shakeri, M. T., 2013, Shear Bond Strength and Antibacterial Effects of Orthodontic Composite Containing TiO_2 Nanoparticles, *Eur. J. Orthod,* 35, 676–679, https://doi.org/10.1093/ejo/cjs073

[12]. Khoroushi, M., Kachuie, M., 2017, Prevention and Treatment of White Spot Lesions in Orthodontic Patients, *Contemp Clin Dent,* Jan-Mar;8(1), 11-19, DOI: 10.4103/ccd.ccd_216_17

[13]. Chambers, C., Stewart, S., Su, B., Sandy, J., Ireland, A., 2013, Prevention and Treatment of Demineralisation During Fixed Appliance Therapy: A Review of Current Methods and Future Applications. *Br. Dent. J,* 215, 505–511, https://doi.org/10.1038/sj.bdj.2013.1094

[14]. Ozak, S. T., Ozkan, P., 2013, Nanotechnology and Dentistry, *Eur. J. Dent,* 7, 145–151, https://doi.org/10.1038/sj.bdj.2013.1094

[15]. Song, W., Ge, S., 2019, Application of Antimicrobial Nanoparticles in Dentistry, *Molecules*, 24, 1033, https://doi.org/10.3390/molecules24061033

[16]. Borzabadi-Farahani, A., Borzabadi, E., Lynch, E., 2014, Nanoparticles in Orthodontics, a Review of Antimicrobial and Anti-Caries Applications, *Acta Odontol. Scand*, 72, 413–417, https://doi.org/10.3109/00016357.2013.859728

[17]. Govindankutty, D., 2015, Applications of Nanotechnology in Orthodontics and Its Future Implications, *Int. J. Appl. Dent. Sci.*, 1, 166–171, https://www.oraljournal.com/pdf/2015/vol1issue4/PartC/1-4-25.pdf

[18]. Varon-Shahar, E., Sharon, E., Zabrovsky, A., Houri-Haddad. Y., Beyth, N., 2019, Antibacterial Orthodontic Cements and Adhesives: A Possible Solution to Streptococcus mutans Outgrowth Adjacent to Orthodontic Appliances, *Oral Health Prev. Dent*, 17, 49–56, search.ebscohost.com

[19]. Sara Dadkan., Mehrdad Khakbiz., Lida Ghazanfari., Meizi Chen., Ki-Bum Lee., 2022, Evaluation of antibacterial and mechanical features of dental adhesives containing colloidal gold nanoparticles. *Journal of Molecular Liquids*, 119824, https://doi.org/10.1016/j.molliq.2022.119824

[20]. Marco Sanchez-Tito., Lidia Yileng Tay., 2024, Effect of The Addition of Silver Nanoparticles on the Mechanical Properties of an Orthodontic Adhesive, *The Saudi Dental Journal*, 36, 359–363, https://doi.org/10.1016/j.sdentj.2023.11.021

[21]. Xu, V. W., Nizami, M. Z. I., Yin, I. X., Yu, O. Y., Lung, C. Y. K, Chu, C. H., 2022, Application of Copper Nanoparticles in Dentistry, *Nanomaterials*, 12(5):805, https://doi.org/10.3390/nano12050805

[22]. Pushpalatha, C., Suresh, J., Gayathri, V. S, Sowmya, S. V., Augustine, D., Alamoudi, A., Zidane, B., Mohammad Albar, N. H., Patil, S., 2022, Zinc Oxide Nanoparticles: A Review on Its Applications in Dentistry. *Front Bioeng Biotechnol*, May 19, 10:917990, https://doi.org/10.3389/fbioe.2022.917990

[23]. Guiar, R. C. O., Nunes, L. P., Batista, E. S., Viana, M. M., Rodrigues, M. C., Bueno-Silva, B, Roscoe, M. G., 2022, Experimental Composite Containing Silicon Dioxide-Coated Silver Nanoparticles for Orthodontic Bonding: Antimicrobial Activity and Shear Bond Strength, *Dental Press J Orthod*, 27(3):e222116, https://doi.org/10.1590/2177-6709.27.3.e222116.oar

[24]. Aguiar, R. C. O., Nunes, L. P., Batista, E. S., Viana, M. M., Rodrigues, M. C., Bueno-Silva, B., Roscoe, M. G., 2022, Experimental Composite Containing Silicon Dioxide-Coated Silver Nanoparticles for Orthodontic Bonding: Antimicrobial Activity and Shear Bond Strength, *Dental Press J Orthod*, 27 (3):e222116, https://doi.org/10.1590/2177-6709.27.3.e222116.oar

[25]. Hasan, L. A., 2021, Evaluation the Properties of Orthodontic Adhesive Incorporated with Nano-Hydroxyapatite Particles, *Saudi Dent J,* Dec;33(8):1190-1196, https://doi.org/10.1016/j.sdentj.2021.01.001

[26]. Mansour, K., Assery, Nancy, Ajwa., Ahoud Alshamrani., Bashayer, J. Alanazi, Bangalore, H., Durgesh, Jukka, P., Matinlinna., 2019, Titanium

Dioxide Nanoparticles Reinforced Experimental Resin Composite for Orthodontic Bonding Mater. *Res*, Express 6, 125098, Doi: 10.1088/2053-1591/ab5a93

[27]. Reddy, A. K., Kambalyal, P. B., Patil, S. R., Vankhre, M., Khan, M. Y., Kumar, T. R., 2016, Comparative Evaluation and Influence on Shear Bond Strength of Incorporating Silver, Zinc Oxide, and Titanium Dioxide Nanoparticles in Orthodontic Adhesive. *J. Orthod.* Sci, 5, 127–131, https://journals.lww.com/joos/_layouts/15/oaks.journals/downloadpdf.aspx?an=01733424-201605040-00004

[28]. Salehi, P., Babanouri, N., Roein-Peikar, M., Zare, F., 2018, Long-Term Antimicrobial Assessment of Orthodontic Brackets Coated with Nitrogen-Doped Titanium Dioxide against Streptococcus Mutans. *Prog. Orthod*, 19, 35, https://link.springer.com/article/10.1186/s40510-018-0236-y

[29]. Sodagar, A., Akhoundi, M. S. A., Bahador, A., Jalali, Y. F., Behzadi, Z., Elhaminejad, F., Mirhashemi, A. H., 2017, Effect of TiO_2 Nanoparticles Incorporation on Antibacterial Properties and Shear Bond Strength of Dental Composite Used in Orthodontics. *Dent. Press J. Orthod*, 22, 67–74, https://doi.org/10.1590/2177-6709.22.5.067-074.oar

[30]. Behnaz, M., Dalaie, K., Mirmohammadsadeghi, H., Salehi, H., Rakhshan, V., Aslani, F., 2018, Shear Bond Strength and Adhesive Remnant Index of Orthodontic Brackets Bonded to Enamel Using Adhesive Systems Mixed with TiO2 Nanoparticles. *Dent. Press J. Orthod*, 23, 43.e1–43.e7, https://doi.org/10.1590/2177-6709.23.4.43.e1-7.onl

[31]. Farzanegan, F., Shafaee, H., Darroudi, M., Rangrazi, A., 2021, Effect of the Incorporation of Chitosan and TiO_2 Nanoparticles on the Shear Bond Strength of an Orthodontic Adhesive: An in Vitro Study, *J. Adv. Oral Res*, 12, 261–266, https://doi.org/10.1177/23202068211015447

[32]. Felemban, N. H., Ebrahim, M. I., 2017, The Influence of Adding Modified Zirconium Oxide-Titanium Dioxide Nano-Particles on Mechanical Properties of Orthodontic Adhesive: An in Vitro Study, *BMC Oral Health*, 17, 43, https://link.springer.com/article/10.1186/s12903-017-0332-2

[33]. Heravi, F., Ramezani, M., Poosti, M., Hossein, M., Shajiei, A., Ahrari, F., 2013, In Vitro Cytotoxicity Assessment of an Orthodontic Composite Containing Titanium-Dioxide Nano-Particles, *J. Dent. Res. Dent. Clin. Dent. Prospect*, 7, 192–198, https://doi.org/10.5681%2Fjoddd.2013.031

[34]. Nasim, I., Kamath, K., Rajeshkumar, S., 2020. Evaluation of the Re-Mineralization Capacity of a Gold Nanoparticle-Based Dental Varnish: An in vitro Study [Internet]. *Journal of Conservative Dentistry.;*23:390. https://doi.org/10.4103%2FJCD.JCD_315_20

[35]. Ying, S., Guan, Z., Ofoegbu, P. C., Clubb, P., Rico, C., He, F., Hong, J., 2022, Green Synthesis of Nanoparticles: Current Developments and Limitations, *Environmental Technology & Innovation*, 26:102336, https://doi.org/10.1016/j.eti.2022.102336

[36]. Aravind Kumar Subramanian, Harsha Lalit, Pugalmani Sivashanmugam, 2023, Preparation, Characterization, and Evaluation of Cytotoxic Activity of a Novel Titanium Dioxide Nanoparticle-infiltrated Orthodontic Adhesive: An in Vitro Study, *World Journal of Dentistry*, 14(10):882-887, https://www.wjoud.com/doi/WJOUD/pdf/10.5005/jp-journals-10015-2319

[37]. Y. Korkmaz, S. Gurgan., E. First., and D. Nathanson., 2010, Effect of Adhesives and Thermocycling on the Shear Bond Strength of A Nano-Composite to Coronal and Root Dentin, *Operative Dentistry*, vol. 35, no. 5, pp. 522–529, https://meridian.allenpress.com/operative-dentistry/article-pdf/35/5/522/1822903/09-185-l.pdf

[38]. Eliasson, S. T., Dahl, J. E., 2020, Effect of Thermal Cycling on Temperature Changes and Bond Strength in Different Test Specimens, *Biomater Investig Dent*, Jan 29;7(1):16-24, Doi: 10.1080/26415275.2019.1709470.

[39]. Aravind, M., Amalanathan, M., Mary, M. S. M., 2021, Synthesis of Tio2 Nanoparticles by Chemical and Green Synthesis Methods and their

Multifaceted Properties, *SN Applied Sciences* 3:409, https://link.springer.com/article/10.1007/s42452-021-04281-5

[40]. Dulger, B., Ozkan, G., Angi, O. S., Ozkan, G., 2024, Green Synthesis of Tio2 Nanoparticles using Aloe Vera Extract as Catalyst Support Material and Studies of their Catalytic Activity in Dehydrogenation of Ethylenediamine Bisborane, *International Journal of Hydrogen* https://doi.org/10.1016/j.ijhydene.2024.02.223

[41]. Pal, M., Garcia Serrano, J., Santiago, P., Pal, U., 2007, Size-Controlled Synthesis of Spherical Tio2 Nanoparticles: Morphology, Crystallization, and Phase Transition, *J PhysChem,* C 111(1):96–102, https://doi.org/10.1021/jp0618173

[42]. Ahmad, M. Z., Alasiri, A. S., Ahmad, J., Alqahtani, A. A., Abdullah, M. M., Abdel-Wahab, B. A., Pathak, K., Saikia, R., Das, A., Sarma, H., Alzahrani, S. A., 2022, Green Synthesis of Titanium Dioxide Nanoparticles using Ocimum sanctum Leaf Extract: In Vitro Characterization and its Healing Efficacy in Diabetic Wounds, *Molecules*, Nov 9;27(22):7712, https://www.mdpi.com/1420-3049/27/22/7712

[43]. Srinivasan, M., Venkatesan, M., Arumugam, V., Natesan, G., Saravanan, N., Murugesan, S., Ramachandran, S., Ayyasamy, R., Pugazhendhi, A., 2019, Green Synthesis and Characterization of Titanium Dioxide Nanoparticles (Tio_2 Nps) Using Sesbania Grandiflora and Evaluation of Toxicity in Zebrafish Embryos, *Process Biochem*, 80:197–202, https://www.academia.edu/download/92621761/j.procbio.2019.02.01020221018-1-aka3st.pdf

[44]. Rajakumar, G., Rahuman, A. A., Roopan, S. M., Khanna, V. G., Elango, G., Kamaraj, C., 2012, Fungus-Mediated Biosynthesis and Characterization of Tio2 Nanoparticles and their Activity Against Pathogenic Bacteria, Spectrochim, Acta, *Part A Mol. Biomol*, Spectrosc, 91:23–29, https://doi.org/10.1016/j.saa.2012.01.011

[45]. K[1] H. T., Balaji Ganesh, S., Devi, R. G., 2020. Colour Stability of Composite Resins-a Review. *Indian Journal of Forensic Medicine & Toxicology*. Oct 29;14(4):4673-8. https://www.researchgate.net/profile/Balaji-Ganeshs/publication/348959167_Colour_Stability_of_Composite_Resins_-A_Review/links/6018d80d45851517ef31fa5e/Colour-Stability-of-Composite-Resins-A-Review.pdf

[46]. Roy Abhinab, C., Kaurani, P., Padiyar, U., Meena, S., Gupta, A., 2021, Effect of Addition of Titanium Oxide and Zirconium Oxide Nanoparticles on the Surface Roughness of Heat Cured Denture Base Resins: An In-Vitro study", *SVOA Materials Science & Technology*, 3(3) Pages: 36-44, https://www.academia.edu/download/67320946/SVOA_MST_03_022.pdf

[47]. Pires, L. A., de Azevedo Silva, L. J., Ferrairo, B. M., Erbereli, R., Lovo, J. F. P., Ponce Gomes, O., Rubo, J. H., Lisboa-Filho, P. N., Griggs, J. A., Fortulan, C. A., et al., 2020, Effects of Zno/TiO2 Nanoparticle and TiO_2 Nanotube Additions to Dense Polycrystalline Hydroxyapatite Bioceramic from Bovine Bones. *Dent. Mater*.;36, e38–e46, https://doi.org/10.1016/j.dental.2019.11.006

[48]. Felemban, N. H., Ebrahim, M. I., 2017, The Influence of Adding Modified Zirconium Oxide-Titanium Dioxide Nano-Particles on Mechanical Properties of Orthodontic Adhesive: An In Vitro Study, *BMC Oral Health*, 17:43, https://link.springer.com/article/10.1186/s12903-017-0332-2